Role of Vibrationally Excited NO in Promoting Electron Emission When Colliding with a Metal Surface: A Nonadiabatic Dynamic Model

Gil Katz,*,†,‡ Yehuda Zeiri,§,|| and Ronnie Kosloff†

Department of Physical Chemistry and the Fritz Haber Research Center, the Hebrew University, Jerusalem 91904, Israel, Department of Chemistry, Northwestern University, Evanston, Illinois 60208-3113, Department of Chemistry, Nuclear Research Center-Negev, P.O. Box 9001, Beer-Sheva 84190 Israel, and Department of Biomedical Engineering, Ben-Gurion University, P.O. Box 653, Beer-Sheva 84105, Israel

Received: April 22, 2005; In Final Form: June 13, 2005

A nonadiabatic quantum dynamic model has been developed to study the process of electron emission from a low-work-function metal surface. The process is initiated by scattering a highly vibrationally excited NO molecule from a surface composed of a Cs layer covering a Ru crystal. The model addresses the increasing quantum yield of the electron emission as a function of the molecular vibrational excitation and incident kinetic energy. The reaction mechanism is identified as a long-range harpooning electron transfer to a molecular ion which is then accelerated toward the surface. Upon impact, the molecular ion emits its excess electron.

I. Introduction

Charge transfer is a key chemical event that is often the driving force behind many catalytic reactions. Heterogeneous catalysis near metal surfaces is no exception. An electron tunneling from the metal valence band to the affinity level of an approaching molecule is in many systems the first step in adsorption and bond dissociation. This is the surface analogue of the gas phase harpooning reaction.[1,2] The work functions of the metal and the molecule electron affinities must therefore play a key role in such reactions. A harpooning mechanism has been suggested for molecules with a high electron affinity, such as the dissociative adsorption of halogens on alkaline metals[3,4] or the dissociation of oxygen on metal surfaces.[5−10] Typically, the reactive products are adsorbed to the surface, but in some cases, when sufficient energy is available, some of the products are emitted to the gas phase. At low incident energies, back electron transfer leads to neutral species.[9,11,12] Higher excitation can lead to ejection of charged particles[13−15] or even free electrons.

Recently, White et al.[16] have reported the observation of electron emission with high quantum efficiency (0.024) when vibrationally excited NO ($\nu = 5-18$) was scattered from a low-work-function (1.3−1.6 eV) metal surface. Does this process follow the same basic charge transfer mechanism found in other adsorbate metal encounters? Harpooning type electron capture would therefore be the first step promoting NO to NO^-. Can this process take place despite the low electron affinity of NO (0.026 eV)?[17] An understanding of these issues clearly requires the development of a suitable theoretical model.

The theoretical framework of describing charge transfer events has been nonadiabatic.[18,19] In the case of gas−metal surface interaction, the Born−Oppenheimer adiabatic separation cannot be justified due to the large number of low-lying electronic excited states associated with the conduction electrons in the metal. Hence, a reliable description of processes involving charge transfer at the gas−solid interface requires knowledge of both ground state and a number of excited state potential surfaces. Accordingly, the time evolution of the system studied has to include possible transition among these potential energy surfaces (PESs), requiring a nonadiabatic quantum dynamical method.[20]

The present theoretical approach simulates the scattering event of a vibrationally highly excited NO molecule, based on three coupled diabatic electronic potential energy surfaces. These surfaces correlate asymptotically to the neutral NO molecule, the NO^- molecular ion, and the NO + e^- products. This description is sufficient for a qualitative understanding of the mechanism of the electron ejection. A more quantitative description should include also the nonadiabatic excitations of electron−hole pairs in the metal as well as an explicit description of additional degrees of freedom. Similar approaches have been used successfully to describe the scattering and the dissociative adsorption mechanisms of O_2 on various metal surfaces.[8,9]

II. The Model

The dynamics of the system is simulated by solving the time-dependent Schrödinger equation on three coupled diabatic potential energy surfaces. The wave packet representing the system is described as a superposition of three wave functions, each residing on a nonadiabatic potential energy surface (PES):

$$\psi = \begin{pmatrix} \psi_g(z,r,\theta) \\ \psi_n(z,r,\theta) \\ \psi_e(z,r,\theta) \end{pmatrix} \tag{1}$$

where z is the NO center-of-mass distance from the surface, r, the internuclear distance, and θ, the orientation angle. The indexes of the wave function projections are g for the gas phase asymptotic NO, n for the negatively charged NO^-, and e for the product NO + e^-. Once an initial state is described, the time propagation is generated by the time-dependent Schrödinger equation:

$$i\hbar \frac{\partial \psi}{\partial t} = \hat{\mathbf{H}}\psi \tag{2}$$

† The Hebrew University.
‡ Northwestern University.
§ Nuclear Research Center-Negev.
|| Ben-Gurion University.

10.1021/jp052107k CCC: $30.25
Published on Web 09/20/2005

where the Hamiltonian is described as

$$\hat{\mathbf{H}} = \begin{pmatrix} \hat{\mathbf{H}}_g & \hat{\mathbf{V}}_{gn} & 0 \\ \hat{\mathbf{V}}_{ng} & \hat{\mathbf{H}}_n & \hat{\mathbf{V}}_{ne} \\ 0 & \hat{\mathbf{V}}_{en} & \hat{\mathbf{H}}_e \end{pmatrix} \tag{3}$$

and $\hat{H}_l = \hat{\mathbf{P}}^2/2\mu + \hat{\mathbf{V}}_l$; l = g, n, e.

The PES were constructed using data from ab initio calculations and adjusted to experimental observations.[17,21] The ground state PES, $\hat{\mathbf{V}}_g$, describes the neutral NO(ν) approaching the metal surface from the gas phase. The molecule is attracted to the surface by a long-range van der Waals force. At short distances, this potential becomes repulsive. During the approach of the molecule to the surface, a charge transfer from the metal to the NO can take place. Such an event leads to the formation of a molecular ion, $NO^-(\nu)$*, which is attracted to the Cs surface by Coulomb attraction to its image charge and described by the potential $\hat{\mathbf{V}}_n$. The possible emission of the electron from the negative molecular ion requires the inclusion of an additional diabatic electronic state that describes a neutral NO interacting with both the Cs surface and a free electron, $\hat{\mathbf{V}}_e$. This PES has the same functional form as the $\hat{\mathbf{V}}_g$ PES but is shifted by the value of the metal work function and the kinetic energy of the electron.[22,23] In what follows, it is assumed that the kinetic energy of the emitted electron is small; hence, it is neglected. The asymptotic energy differences between the three electronic states is therefore determined by the NO electron affinity and the metal work function.

The dynamics of the scattering process is studied using a reduced dimensionality model with two degrees of freedom.

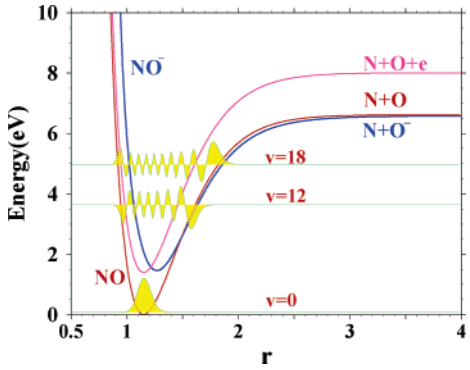

Figure 1. Potential energy as a function of the internuclear distance, r, representing an asymptotic cut ($Z = \infty$) of the three potential surfaces—NO, NO^-, and NO + e. Three initial vibrational states of NO are superimposed on the PES: $\nu = 0$, $\nu = 12$, and $\nu = 18$.

TABLE 1: Parameters of the NO−Cesium Potential (Energy in eV, Distance in Å)

	Physisorption		
$A_g = 829$	$C_g^0 = 4.2$	$b_g = 3.73$	$z_e = 2.217$
$D_g = 6.614$	$r_e^g = 1.159$	$r_e^{ad} = 1.1$	
$a_{1NO}^g = 5.398$	$a_{2NO}^g = 7.041$	$a_{3NO}^g = 4.823$	
$a_{1NO}^{ad} = 5.67$	$a_{2NO}^{ad} = 7.5$	$a_{3NO}^{ad} = 4.17$	
$C_{6NO} = 3.8$	$C_{8NO} = 2.1$	$C_{10N-O} = 1.5$	
$Z_{efc}^g = 0$	$Z_{efc}^{ad} = 0.1$		
	NO^-		
$A_m^{(M-NO^-)} = 2.2$	$b_m = 3.13$	$\alpha_{M-NO^-} = 0.7$	$z_e = 2.01$
$D_g = 5.14$	$r_e^g = 1.273$	$r_e^{ad} = 1.2$	
$a_{1NO^-}^{ad} = 5.37$	$a_{2NO^-}^g = 7.504$	$a_{3NO^-}^g = 1.78$	
$a_{1NO^-}^{ad} = 5.69$	$a_{2NO^-}^{ad} = 8.16$	$a_{3NO^-}^{ad} = 1.61$	
$C_{4NO^-} = 3.3$	$C_{6NO^-} = 4.7$	$C_{8NO^-} = 1.67$	
$Z_{efc}^{ad} = -0.9$	$Z_{efc}^g = -1$	$E_m = 1.4$	$E_a^{NO} = 0.026$

The two coordinates explicitly considered are the molecular center-of-mass distance from the surface, z, and the molecular interatomic distance, r. The rotational degrees of freedom of the molecules are neglected in the present calculation, and therefore, a flat orientation is assumed. Within the degrees of freedom considered in the model, the potential energy is cast into an analytic functional form adopted from ref 24. The parameters used in the potential function for the different species are fit to ab initio calculations and experimental data. The van der Waals attraction between the neutral molecule at long distances and repulsive forces at short distances are cast into the Born−Meyer potential form. At short z values, the NO molecule becomes slightly positively charged by Z_{efc}^{NO}. As a result, the molecule has an additional Coulomb attraction to its image in the surface. The internal molecular potential is described by a form suggested by Murrell for diatomic molecules.[24] These considerations lead to the PES function of the neutral NO interacting with the metal surface:

$$\mathbf{V}_g(r,z,\theta) = A_g e^{-b_g z} - \frac{C_g(\theta)}{z^3}\xi_4 - \frac{Z_{efc}^{NO}(z)}{2z}\xi_2 + D_g[1 + a_{1NO}(z)q + a_{2NO}(z)q^2 + a_{3NO}(z)q^3]e^{-a_{1NO}(z)(q)} - \frac{(C_{6NO}(z)\xi_6}{q^6} + \frac{C_{8NO}(z)\xi_8}{q^8} + \frac{C_{10NO}(z)\xi_{10}}{q^{10}} \tag{4}$$

where θ is the orientation angle between r and z, $q = (r - r_e(z))$ and $\xi_n = (1 - \Gamma_n(r, 0, 2a_1))$. The function $C_g(\theta)$ has the following form: $C_g(\theta) = C_g^0 + C_g^2 P_2(\cos(\theta))$, where $P_2(X)$ is the second Legendre polynomial. In the following, a flat surface is assumed; therefore, the angular dependence and the translation along the surface are neglected ($C_g^2 = 0$). The incomplete Gamma function, Γ_n, is used to interpolate the potential parameters. In the gas phase, its value is $\Gamma_n = 0$ and near the surface $\Gamma_n = 1$:

$$\Gamma_n(z,z_0,a) = \sum_{k=0}^{k=m}\left[\frac{a(z - z_0)^k}{k!}\right]e^{-a(z-z_0)} \tag{5}$$

The interpolation form is chosen as

$$Q_{NO}(z) = Q_{NO}^{ad} \quad \text{for} \quad z < z_e$$

$$Q_{NO}(z) = Q_{NO}^{g} - (Q_{NO}^{g} - Q_{NO}^{ad})\Gamma_n(z,z_e,b_g) \quad \text{for} \quad z > z_e \tag{6}$$

where the interpolated potential parameters are $Q = r_e$, a_j, or Z_{efc}. The position of the solid surface, z_0, was chosen to be zero.

The molecular ion PES describes a combination of direct binding to the surface represented by a Morse potential with an additional Coulomb interaction with the image charge in the metal. The molecular ion internal potential is cast in the same form suggested by Murrell.[24] Thus, the PES for the NO^-/Cs becomes

$$\mathbf{V}_m(r,z) = A_m^{(M-NO^-)}(1 - e^{-\alpha_{M-NO^-}(r)(z-z_e)})^2 - \frac{Z_{efc}^{NO^-}(z)}{2z}(\xi_2) + D_a^{(NO^-)}[1 + a_{1NO^-}(z)q + a_{2NO^-}(z)q^2 + a_{3NO^-}(z)(q)^3]e^{-a_{1NO^-}(z)(q)} - \frac{(C_{4NO^-}(z)\xi_4}{q^4} + \frac{C_{6NO^-}(z)\xi_6}{q^6} + \frac{C_{8NO^-}(z)\xi_8}{q^8} + E_m - E_a^{NO} \tag{7}$$

The interpolation of potential parameters from the gas phase to

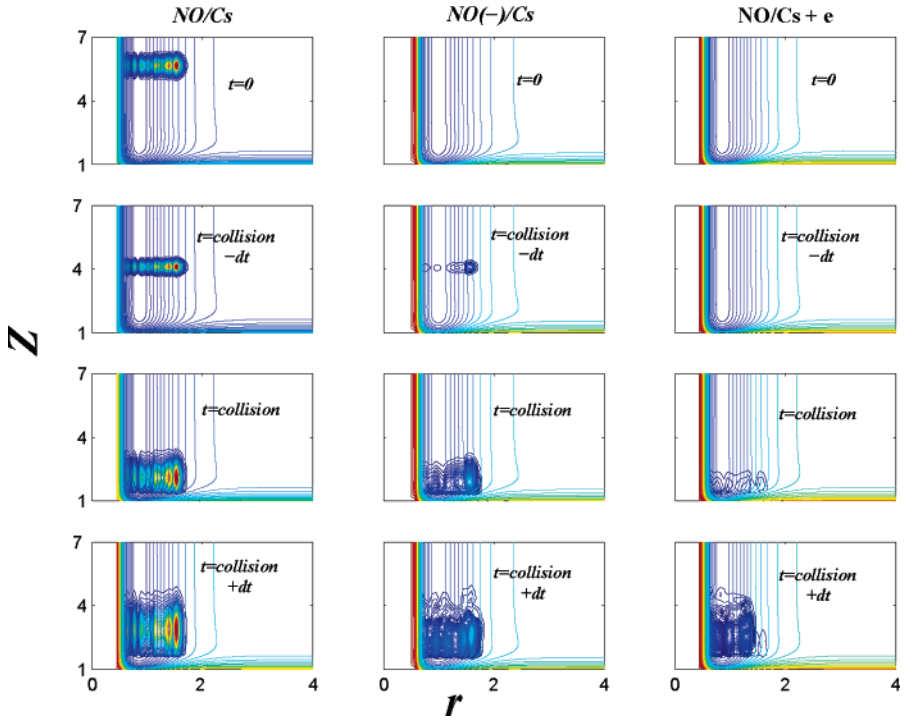

Figure 2. Snapshots of the wave function showing the sequence of events leading to electron emission. The top panel shows the initial wave packet at $t = 0$. Amplitude can only be found on the NO PES where the initial vibration is $\nu = 14$ and $E_k = 0.5$ eV. The second panel shows the wave function at d$t = 10$ fs. Amplitude starts to appear on the NO^- PES. Panel 3 shows the collision time of $t = 20$ fs. More amplitude is converted to NO^- as well as appearance of electron emission. Panel 4 shows the outgoing wave packet after 30 fs. Significant amplitude is seen on the electron emission PES $\hat{V}_e$. The distances are in angstroms.

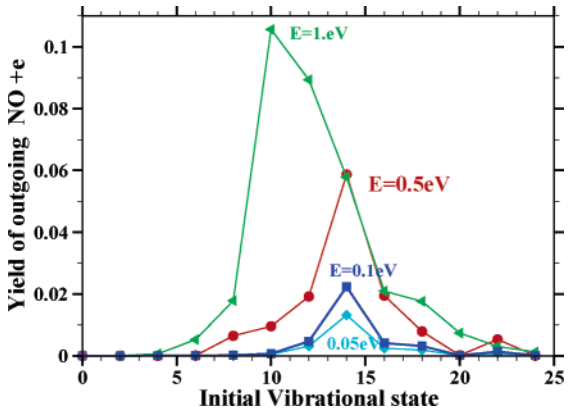

Figure 3. Accumulated flux on the PES representing electron emission as a function of the initial vibrational state and different incident kinetic energies.

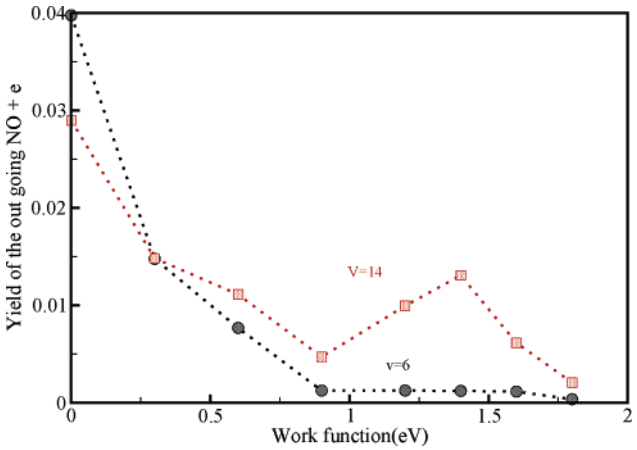

Figure 4. Reaction yield as a function of the surface work function. The initial vibrational state $\nu = 6$ is indicated by circles and $\nu = 14$ by squares.

the adsorbed position was done using eq 6. The bond equilibrium distances and the vibrational frequencies of the NO molecule and molecular ion in the gas phase were calculated using density functional theory (DFT). The B3LYP approximation for the exchange correlation term was used in the calculation together with the 6−31G** basis set.[25] The present DFT calculations on NO^- are consistent with earlier ones of McCarthy et al.[17] These calculations are in good agreement with experimental data of gas phase NO,[26] for example, a vibrational frequency of 1904 cm^{-1} compared to the calculated 1920 cm^{-1} as well as an equilibrium distance of $r_e = 1.1508$ Å compared to the calculated 1.159 Å. Larger errors are found in dissociation energies; the experimental value is $D_0 = 6.14$ eV compared to the calculated $D_0 = 5.8$ eV. The asymptotic difference between the NO^- and NO curves is the electron affinity of oxygen. The calculated DFT value is 1.6 eV in comparison to the experimental value of 1.4 eV. These results give an estimate of the upper bound on the error in the calculated PES of ∼0.2 eV.

The variations of the molecular parameters due to adsorption were estimated by performing DFT calculations on the Cs−NO molecule and comparison to the calculations by Orita et al.[27] on the interaction of NO with Ni and Pd surfaces. The ground state of the molecule near the surface as calculated in DFT is partially negatively charged. This causes an increase in the vibrational frequency from 1275 to 1612 cm^{-1}. The adsorbed neutral NO is partially positively charged. The result is an increase in vibrational frequency of 100 cm^{-1}. The gas phase NO^+ parameters used in the interpolation are adopted from ref 28. Table 1 summarizes the potential parameters used in the simulation. The parameters were chosen to fit the PES to ab initio calculations and the experimental data described above.

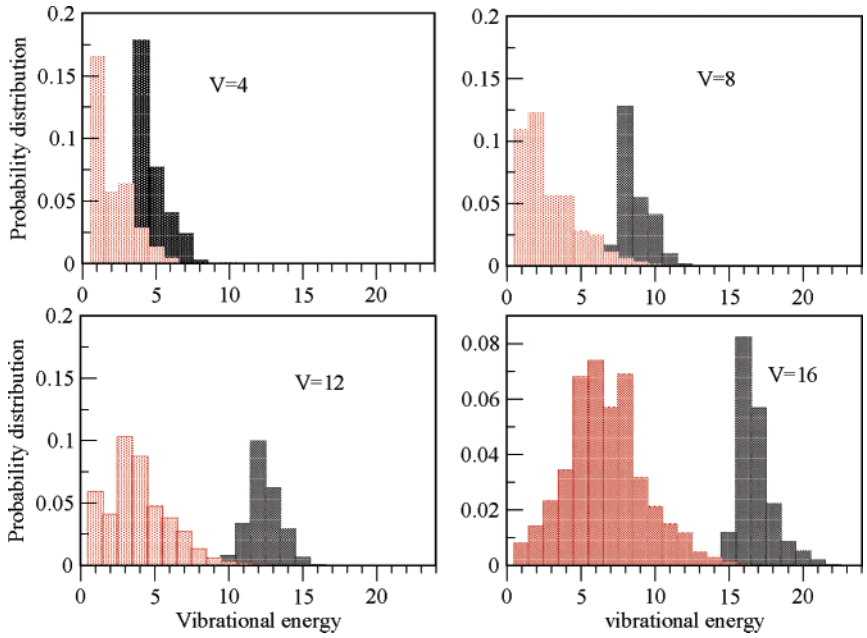

Figure 5. Vibrational distribution of the outgoing nonreactive NO and the reactive NO + e^- (NO + e^-, red; NO, black). Four different initial vibrational states are shown for $E_k = 0.5$ eV.

On these potentials, the vibrational eigenvalues were calculated by the relaxation scheme and compared to the experimentally measured frequencies of the different gas phased species, 1920 cm^{-1} for the neutral NO and 1275 cm^{-1} for the NO^-. Figure 1 shows the three asymptotic molecular potentials for a metal with a work function of 1.4 eV.

The free parameters in the model are the off-diagonal nonadiabatic coupling terms. These terms are chosen to be proportional to the local electron density[8] which tunnels to the vacuum

$$\boldsymbol{V}_{ab}(z,r) = A_{ab} e^{-\alpha_{int} z/\hbar} \tag{8}$$

The decay parameter, α_{int}, is a function of the effective charge differences between the diabatic states, $\alpha_{int} = \sqrt{(-2(E_m)|Z^a_{efc} - Z^b_{efc}|)/m_e \cdot e}$, where Z^i_{efc} is the effective charge of species i and E_m is the Cs work function (typically 1.4 eV). The value of A_{ab} was set as $A_{ab} = 0.45$ eV for all the nonadiabatic coupling terms. In the region of small coupling, relevant for this study, the total transition probability from one surface to the other is proportional to A^2_{ab}; this means that the value of A_{ab} could be fit to the total electron emission yield.[10,29] The quantum dynamics of the encounter was simulated by solving the multichannel time-dependent Shcrödinger equation.[10] The initial wave function was constructed as a product of a plane wave describing the motion of NO toward the surface and a vibrational eigenstate. These NO vibrational eigenstates were calculated using the relaxation method.[30] Three vibrational wave functions are shown in Figure 1. This initial product wave function was then propagated using the Chebychev scheme.[31] The propagation was stopped when the wave function completed the collision. Analysis of the scattering process was carried out by integrating the flux at the asymptotic region of the channel, leading to electron emission.[32]

III. Results and Discussion

A typical sequence of events leading to electron emission is displayed in Figure 2. Initially, at $t = 0$, the wave function has amplitude only on the NO PES, $\hat{\mathbf{V}}_g$. This wave function accelerates toward the surface. Still on its way in, the wave function reaches a distance where the nonadiabatic coupling is sufficiently strong to transfer amplitude to the NO^- PES, $\hat{\mathbf{V}}_n$. This electron transfer event takes place at the outer vibrational turning point where the two potentials cross each other. The wave packet continues to accelerate toward the surface until it reaches the repulsive part of the potential. The curvature of the potential at this region can mix the translational and vibrational degrees of freedom. This allows amplitude to be transferred to the electron emission PES $\hat{\mathbf{V}}_e$ which requires converting incident vibrational energy to overcome the metal work function. As a result, the vibrational energy of the outgoing emission wave function is reduced (cf. Figures 2 and 5).

The calculation shown in Figure 2 was repeated for different initial vibrations and incident kinetic energy. The accumulated fluxes of the outgoing electron emission wave packet are displayed in Figure 3. The results show a growth of the reaction yield with an increase in vibrational energy, reaching a maximum at $\nu = 14$ for low incident kinetic energy. These results are consistent with the experiments that were carried out for $\nu = 18$ and low incident kinetic energy.[16] At higher incident energies, the maximum shifts to lower vibrational states ($\nu = 8$ for $E_k = 1$ eV). This observation reflects the fact that at higher kinetic energy the mechanism changes and most of the nonadiabatic transfer occurs upon impact with the repulsive part of the PES.

The vibrational distribution of the NO molecule ejected back to the gas phase is displayed for the reactants and the products in Figure 5. The vibrational cooling of the product NO yielding electron emission is clearly seen.

The effect of varying the value of the metal work function was also investigated, as is displayed in Figure 4. For high initial vibrational numbers, a maximum in electron emission is found when the metal work function is matched by the electron affinity of oxygen. In this case, the nonadiabatic transfer takes place upon approach at large distances from the surface. For lower vibrational excitation, most of the reaction takes place upon impact. Therefore, the electron emission is maximized at low work function values.

The present simulation ignores the possible excitation of electron−hole pairs in the metal as well as the kinetic energy of the emitted electrons. A treatment of these effects has to be undertaken in the context of an open quantum system.[33,34] Li and Guo[34] carried out a study of vibrational relaxation of NO near a metal surface. The calculation included coupling to electron−hole pairs in the metal modeled by a Monte Carlo wave packet approach. The simulation method is a stochastic realization of Lindblad semigroup dynamics.[33,35] Only two electronic surfaces were included, the NO/surface and the NO^-/surface. For this reason, the possibility of electron emission was excluded. The calculation modeled a metal surface such as Cu with a work function of ∼4.7 eV. Since this value is much higher than the present Cs covered Ru surface of 1.4 eV, the electron emission channel was energetically closed in the energy range considered by Li and Guo. One of the main results of their study was that the transitions between the two electronic surfaces were in close vicinity of the crossing seam. Due to the high value of the work function, this seam was located close to the surface with a curvature which facilitated vibration to translation transfer. In the present case of a surface with a low work function, the crossing seam is almost parallel to the vibration and extends far out into high z values. In agreement with the results of Li and Guo and with calculations on the influence of dissipation on the charge transfer reactions of O_2 on metals,[29] dissipation due to electron−hole pairs does not alter the qualitative features of the crossing dynamics which takes place predominantly near the crossing seam.

An alternative mechanism of electron emission due the creation of a local hot spot will require partial equilibration of the incoming molecule and the surface. The time scale of such a process requires temporary trapping of the NO on the surface. Such a process will lead to a very different product, vibrational and translational distributions which are only correlated to the incident energy.

Considering the influence of the excitation of electron−hole pairs on the direct mechanism of electron emission, the loss of effective energy available for the reaction will result in a lower yield. NO colliding with high- and low-work-function metals will lead to significant vibrational relaxation. The difference is the prediction of a bimodal vibrational distribution of the products (cf. Figure 5) when the electron emission channel is open. It is expected that dissipation will broaden these distributions and shift them to slightly lower energy.

Calculations with other potential forms have been carried out. The general qualitative trends have been reproduced. The curvature of the potential upon impact which is able to transform vibrational energy into electronic energy is clearly important. For example, a steeper repulsive part on the NO^-/surface PES, $\hat{\mathbf{V}}_g$, was found to enhance the electron emission. In addition, it is expected that the perpendicular orientation of NO with respect to the surface normal will promote the electron emission. When the molecular repulsive part of the NO^- potential is softer, a second curve crossing seam appears between $\hat{\mathbf{V}}_n$ and $\hat{\mathbf{V}}_e$ located near the inner vibrational turning point. Such a seam allows long-range curve crossing from the NO^- PES, $\hat{\mathbf{V}}_n$, to the NO + e PES, $\hat{\mathbf{V}}_e$. The current potentials do not support such a mechanism. The present mechanism also points to the predominant role that incident vibrational excitation plays compared to translation in promoting electron emission.

To conclude, the quantum nonadiabatic simulation of the electron emission from vibrationally excited NO from a metal surface reveals a mechanism composed of a long-range electron transfer to NO^- which emits its electron upon impact. These calculations are in qualitative agreement with the experimental observations of White et al.[16]

Acknowledgment. We thank Dan Auerbach for helpful discussions and sharing with us the experimental results of ref 16 prior to publication. This research was supported by the German-Israel Foundation (GIF). The Fritz Haber Research Center is supported by the Minerva Gesellschaft für die Forschung, GmbH München, FRG.

References and Notes

(1) Ogg, R. A. J.; Polanyi, M. *Trans. Faraday Soc.* **1935**, *31*, 604.
(2) Evans, M. G.; Polanyi, M. *Trans. Faraday Soc.* **1938**, *34*, 11.
(3) Kasemo, B. *Phys. Rev. Lett.* **1979**, *32*, 1114.
(4) Hellberg, L.; Stromquist, J.; Kasemo, B.; Lundqvist, B. I. *Phys. Rev. Lett.* **1995**, *74*, 4742.
(5) Reijnen, P. H. F.; Raukema, A.; Van Slooten, U.; Kleyn, A. W. *Surf. Sci.* **1991**, *253*, 24.
(6) Vattoune, L.; Rocca, M.; Boragno, C.; Valbusa, U. *J. Chem. Phys.* **1994**, *101*, 713.
(7) Greber, T. *Surf. Sci. Rep.* **1997**, *28*, 1.
(8) Katz, G.; Zeiri, Y.; Kosloff, R. *Surf. Sci.* **1999**, *425*, 1−14.
(9) Kosloff, R.; Katz, G.; Zeiri, Y. *Faraday Discuss.* **2000**, *117*, 291−301.
(10) Katz, G.; Zeiri, Y.; Kosloff, R. *J. Chem. Phys.* **2004**, *120*, 3931−3948.
(11) Komorowski, A. J.; Sexton, J. Z.; Kummel, A. C.; Binetti, M.; Weise, O.; Hasselbrink, E. *Phys. Rev. Lett.* **2001**, *87*, 246103.
(12) Komorowski, A. J.; Ternow, H.; Razaznejad, B.; Bernbak, B.; Sexton, J. Z.; Zoric, I.; Kasemo, B.; Lundqvist, B. I.; Kleyn, A. W.; Kummel, A. C. *J. Chem. Phys.* **2002**, *117*, 8185.
(13) Danon, A.; Amirav, A. *Phys. Rev. Lett.* **1990**, *65*, 2038.
(14) Danon, A.; Amirav, A. *J. Phys. Chem.* **1989**, *93*, 5549.
(15) Kleyn, A. W. *The Physics of Electronic and Atomic Collisions*, 1978; p 451.
(16) White, J. D.; Chen, J.; Matsiev, A.; Aurbach, D. J.; Wodtke, A. M. *Nature* **2004**.
(17) McCarthy, M. C.; Allington, J. W. R.; Griffith, K. S. *Chem. Phys. Lett.* **1998**, *289*, 156.
(18) Zener, C. *Proc. R. Soc. London, Ser. A* **1932**, *137*, 696.
(19) Landau, L. D. *Phys. Sowjetunion, Z.* **1932**, *1*, 46.
(20) Jorgensen, S.; Dubnikova, F.; Zeiri, Y.; Kosloff, R.; Lilach, Y.; Asscher, M. *J. Phys. Chem. B* **2004**, *108*, 14056−1406.
(21) Huang, Y. H.; Rettner, C. T.; Aurbach, D. J.; Wodtke, A. M. *Science* **2000**, *290*, 111.
(22) Meier, C.; Engel, V. *J. Chem. Phys.* **1994**, *101*, 2673.
(23) Grafe, S.; Scheidel, D.; Engel, V.; Henriksen, N. E.; Moller, K. B. *J. Phys. Chem. A* **2004**, *108*, 8954−8960.
(24) Huxley, P.; Murrell, J. N. *J. Chem. Soc., Faraday Trans. 2* **1983**, *79*, 323.
(25) Frisch, M. J.; et al. *Gaussian 03*, revision C.02; Gaussian, Inc.: Wallingford, CT, 2004.
(26) Huber, K. P.; Hertzberg, G. *Molecular Spectra and Molecular Structure IV of Diatomic Molecules*; Van Nostrnad Reinhold Company: New York, 1979.
(27) Orita, H.; Nakamura, I.; Fujitani, T. *J. Chem. Phys.* **2005**, *122*, 014703.
(28) Bowman, W. C.; Herbst, E.; DeLucia, F. C. *J. Chem. Phys.* **1982**, *77*, 4261.
(29) Katz, G.; Zeiri, Y.; Kosloff, R. *Isr. J. Chem.* **2005**, *45*, 27.
(30) Kosloff, R.; Tal-Ezer, H. *Chem. Phys. Lett.* **1986**, *127*, 223−230.
(31) Tal Ezer, H.; Kosloff, R. *J. Chem. Phys.* **1984**, *81*, 3967−3970.
(32) Katz, G.; Baer, R.; Kosloff, R. *Chem. Phys. Lett.* **1995**, *239*, 230−236.
(33) Koch, C. P.; Klüner, T.; Freund, H.-J.; Kosloff, R. *Phys. Rev. Lett.* **2003**, *90*, 117601.
(34) Li, S. M.; Guo, H. *J. Chem. Phys.* **2002**, *117*, 4499.
(35) Saalfrank, P.; Kosloff, R. *J. Chem. Phys.* **1996**, *105*, 2441.